

Cite this: *Chem. Commun.*, 2011, **47**, 7617–7619

www.rsc.org/chemcomm

## COMMUNICATION

## Isomerically pure electron-deficient anthradithiophenes and their acceptor performance in polymer solar cells†

Zhong Li,<sup>a</sup> Yee-Fun Lim,<sup>b</sup> Jong Bok Kim,<sup>c</sup> Sean R. Parkin,<sup>a</sup> Yueh-Lin Loo,<sup>c</sup> George G. Malliaras<sup>bd</sup> and John E. Anthony<sup>\*a</sup>

Received 25th April 2011, Accepted 24th May 2011

DOI: 10.1039/c1cc12410b

Amide functionalized anthradithiophenes (ADTs) play active acceptor roles in polymer bulk-heterojunction solar cells. The first separation of ADT isomers is reported, and the regiochemistry of the ADT has significant impact on crystal packing and solar cell performance. Cell efficiency up to 0.80%, due in large part to high open-circuit voltage ( $V_{OC} > 1.0$  V), is achieved in bulk-heterojunction solar cells comprising *syn*-ADT and poly(3-hexylthiophene).

The fast-growing field of bulk heterojunction (BHJ) polymer solar cells<sup>1</sup> has gained enormous attention in recent years. Since the new millennium, significant progress in the understanding of fundamental device physics,<sup>2</sup> the discovery of new materials<sup>3</sup> and the invention of new processing protocols<sup>4</sup> triggered a series of impressive gains in power conversion efficiencies (PCEs). Some of the greatest strides have arisen from new high-performance low-band-gap polymer donors, yielding PCE over 7%.<sup>5</sup> In contrast, the development of new acceptors has been sluggish, with [6,6]-phenyl-C<sub>61</sub>-butyric acid methyl ester (PC<sub>61</sub>BM)<sup>6</sup> and related derivatives<sup>7</sup> still dominating the field after more than 15 years. In the past few years, research activities on non-fullerene acceptors, whether small molecules<sup>8</sup> or polymers,<sup>9</sup> have become more common. This class of acceptors has interesting potential, with convenient synthesis, low cost, easy tunability of energy levels, and perhaps most importantly, better absorption in the visible spectrum. Small molecule acceptors have received particular attention, as shown by the work on perylene diimides,<sup>10</sup> Vinazenes,<sup>11</sup> diketo-pyrrolopyrrole<sup>12</sup> and bifuorenylidene.<sup>13</sup>

Based on our previous studies on acene-based electron donors,<sup>14</sup> we have extended our research to acceptor materials

by preparing electron-deficient pentacenes,<sup>15</sup> some of which<sup>16</sup> are among the best small molecule acceptors for BHJ polymer solar cells. More importantly, we have found that there is a correlation between the crystal structure of acene-based acceptors and cell performance, with a unique “sandwich herringbone” structure yielding the best PCE (~1.5%) in bulk-heterojunction devices with poly(3-hexylthiophene) (P3HT). Encouraged by these results, we reasoned that the well-studied heteroacene anthradithiophene (ADT) may be even more interesting due to its better ambient stability. In this communication, we report on the synthesis and characterization of *isomerically-pure* electron-deficient ADT amides (ADTAs), namely *syn*-ADTA and *anti*-ADTA (Fig. 1), and their solar cell performance in both bulk- and planar-heterojunction devices with P3HT.

ADTs are usually prepared and studied as inseparable mixtures of the *syn*- and *anti*-regioisomers, and the precursors of the ADTAs in this study, including the quinone, dibromide, dicarboxylic acid and diacid chloride, were prepared as such mixtures (Scheme S1, ESI†). The as-synthesized amide (*mix*-ADTA) was also a mixture showing no sign of isomer separation on silica gel thin layer chromatography. However, it was noted that in certain solvents, such as toluene and chlorobenzene, *syn*- and *anti*-ADTAs crystallized independently out of the isomer mixture to form distinct crystals (Fig. 1). Thus,

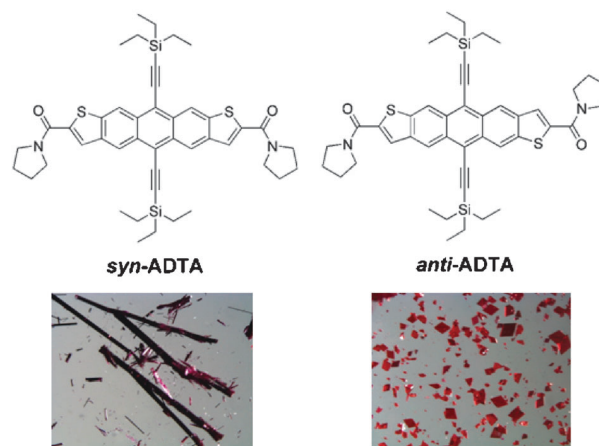


Fig. 1 Molecular structures and optical images of the crystals of *syn*- and *anti*-ADTAs.

<sup>a</sup> Department of Chemistry, University of Kentucky, Lexington, KY 40506, USA. E-mail: anthony@uky.edu

<sup>b</sup> Department of Materials Science and Engineering, Cornell University, Ithaca, NY 14850, USA

<sup>c</sup> Department of Chemical and Biological Engineering, Princeton University, Princeton, NJ 08544, USA

<sup>d</sup> Centre Microelectronique de Provence, Ecole Nationale Supérieure des Mines de Saint Etienne, 880, route de Mimet, 13541 Gardanne, France

† Electronic supplementary information (ESI) available: Experimental details, synthetic procedures, crystallographic CIF files and additional supportive data. CCDC 824023 and 824024. For crystallographic data in CIF or other electronic format see DOI: 10.1039/c1cc12410b

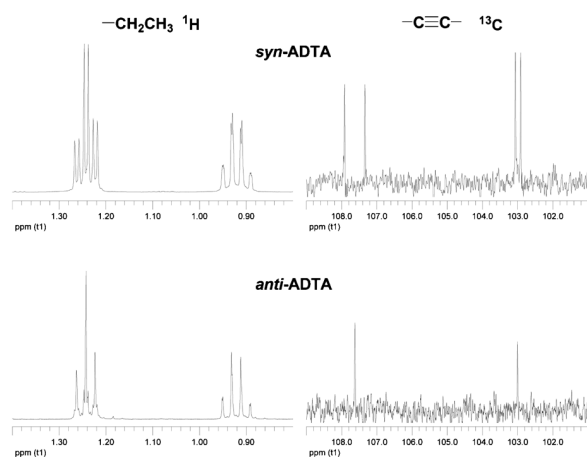


Fig. 2 Differences in the NMR spectra of *syn*- and *anti*-ADTAs.

gram-scale isomerically-pure ADTAs could be easily obtained using a simple, scalable fractional crystallization process. The differential solubility of the isomers is likely a result of a difference in dipole moment—calculations (Fig. S2, ESI<sup>†</sup>) estimate the dipole moment of *syn*-ADTA (8.87 Debye) to be significantly larger than the *anti* counterpart (0.02 Debye).

The spectroscopic and electronic characteristics of these two isomers are quite similar. The <sup>1</sup>H and <sup>13</sup>C NMR spectra of the two isomers differ only in the proton signals for the triethylsilyl groups, and in the carbon signals for the alkyne (Fig. 2). Both isomers yield an electrochemically estimated HOMO at  $-5.34$  eV and LUMO at  $-3.21$  eV vs. vacuum (Fig. S7, ESI<sup>†</sup>), and absorption spectra exhibit small differences only in the near-UV region. Compared to PC<sub>61</sub>BM, which has poor absorption in the visible spectrum, ADTAs exhibit intense absorption between 500–700 nm (Fig. S7B, ESI<sup>†</sup>). Since P3HT absorbs mostly in the same window (Fig. S8, ESI<sup>†</sup>), in principle ADTAs could pair with other low-band gap polymer donors to capture more visible light.

In contrast to their electronic properties, the crystal packing of the isomers was found to vary depending on the regio-chemistry of thiophene moieties, as already indicated by the different crystal forms noted during purification (Fig. S1, ESI<sup>†</sup>). Single crystal X-ray analysis revealed that *syn*-ADTA adopts a triclinic crystal structure with two ADTAs and two toluene molecules per unit cell. The two ADTA molecules are related by inversion with strong  $\pi$ - $\pi$  interaction ( $\sim 3.4$  Å) and opposing dipole moments, resulting in a strong 1-D  $\pi$ -stacking motif (Fig. 3A). However, *anti*-ADTA forms twinned crystals without the incorporation of solvent. A herringbone packing motif was observed, with *no*  $\pi$ - $\pi$  interactions between molecules because of the complete facial offset of adjacent ADT cores (Fig. 3B).<sup>‡</sup> Clearly, the remarkable difference in crystal



Fig. 3 Crystal packing of *syn*-ADTA (A) and *anti*-ADTA (B). Ethyl groups omitted for clarity.

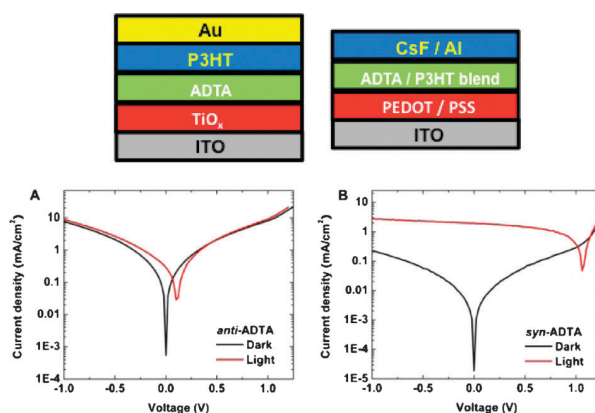


Fig. 4 Top: planar (left) and BHJ (right) device configurations. Bottom:  $J$ - $V$  curves of *anti*-ADTA (A) and *syn*-ADTA (B) BHJ solar cells.

packing suggests completely different transport properties for the isomers.

In most literature work, ADT derivatives were studied as *syn/anti* mixtures due to the great challenge in the preparation of isomerically pure materials. Although excellent device properties were still achieved,<sup>17</sup> the impact of isomeric impurity on materials properties remains unclear. There are several reports of other heteroacenes<sup>18</sup> addressing the correlation of regio-isomers and charge mobilities when tested in thin film transistors, but such studies have not been carried out on ADT-based materials.

We evaluated the acceptor properties of *syn*-, *mix*- and *anti*-ADTAs in both planar- and BHJ solar cells (Fig. 4), and we indeed observe significant performance differences based on the isomer configuration and isomeric purity (Table 1). In planar heterojunction devices, the cell performance of the three acceptors is low due to the limited charge separation interface, but devices with *syn*-ADTA still clearly outperformed those with *anti*-ADTA by a factor of about three in PCE, mainly due to differences in photocurrent. In the BHJ architecture, an even greater contrast was seen. Compared to the barely functioning devices comprised of the *anti*-isomer, *syn*-ADTA yielded much better cell efficiency, up to 0.8%. Furthermore, *mix*-ADTA yielded a device performance intermediate between the pure isomers. Most likely, when this statistical mixture is used, *anti*-ADTA behaves essentially as an inactive impurity, forming poorly-functioning crystalline domains that hinder charge transport. This effect is much

Table 1 Solar cell performance of *syn*-, *mix*- and *anti*-ADTAs

	$V_{oc}/V$	$J_{sc}/mA\ cm^{-2}$	FF	PCE (%)
No annealing (planar)				
<i>syn</i>	$0.98 \pm 0.01$	$0.31 \pm 0.01$	$0.30 \pm 0.01$	$0.091 \pm 0.001$
<i>mix</i>	$0.98 \pm 0.01$	$0.29 \pm 0.02$	$0.29 \pm 0.01$	$0.084 \pm 0.006$
<i>anti</i>	$0.88 \pm 0.01$	$0.14 \pm 0.01$	$0.29 \pm 0.01$	$0.035 \pm 0.002$
Before thermal annealing (BHJ)				
<i>syn</i>	$0.88 \pm 0.05$	$1.31 \pm 0.12$	$0.31 \pm 0.01$	$0.36 \pm 0.03$
<i>mix</i>	$0.59 \pm 0.08$	$0.72 \pm 0.21$	$0.29 \pm 0.01$	$0.13 \pm 0.05$
<i>anti</i>	$0.06 \pm 0.01$	$0.30 \pm 0.04$	$0.25 \pm 0.02$	$0.004 \pm 0.001$
After thermal annealing at 120 °C for 1 min (BHJ)				
<i>syn</i>	$1.05 \pm 0.01$	$1.93 \pm 0.10$	$0.39 \pm 0.01$	$0.80 \pm 0.04$
<i>mix</i>	$0.59 \pm 0.03$	$0.55 \pm 0.10$	$0.28 \pm 0.01$	$0.09 \pm 0.01$
<i>anti</i>	$0.10 \pm 0.01$	$0.30 \pm 0.02$	$0.26 \pm 0.03$	$0.008 \pm 0.001$

more profound in BHJ cells, presumably as a reflection of the strong dependence of cell performance on subtle morphology changes in the active layer. The issue is likely exacerbated by the differential rate of crystallization of the two ADTA isomers, which will have a dramatic impact on phase separation.

The impact of blend morphology is also the driving force for the dramatic difference in the  $V_{oc}$  of test cells fabricated in the BHJ configuration. The identical LUMO energies of the two isomers make this difference unusual, since  $V_{oc}$  is typically estimated based on the energy offset between the donor HOMO and the acceptor LUMO.<sup>19</sup> However, a more recent equation derived by Kippelen and co-workers which correlates  $V_{oc}$  to  $\ln(J_{sc}/J_{dark})$  seems to better describe our results.<sup>20</sup> For **anti-ADTA**, larger scale aggregation was observed in the blend film (Fig. S9A, ESI<sup>†</sup>), resulting in pinholes and higher dark current that is believed to be responsible for its lower  $V_{oc}$  (Fig. 4A). On the other hand, films of **syn-ADTA**/P3HT show a more uniform coverage textured with small grains of the acceptor (Fig. S9B, ESI<sup>†</sup>), yielding a lower  $J_{dark}$  and leading to a  $V_{oc}$  commensurate to its estimated LUMO (Fig. 4B). Although the Kippelen equation was originally based upon bilayer cells, our results indicate its viability in BHJ cells.

Consistent with results from other small-molecule acceptors,<sup>13</sup> the electrochemically derived LUMO for our acceptor is nearly identical to that reported for P3HT (−3.2 eV). Of course, electrochemical measurements are only rough estimates of the energy levels, and there may indeed be significant offset between the two LUMO levels. A detailed exploration of the impact of small changes in ADTA LUMO energy on device current, as well as manipulating substituents to induce the “sandwich herringbone” crystal packing motif we found beneficial in pentacene acceptors, are targets for materials under development.

In conclusion, we have demonstrated that the introduction of amide groups to ADTs has not only converted these p-type materials into novel acceptors that can be used in organic solar cells, it also caused differential self-assembly of the *syn*- and *anti*-isomers that allowed for the first time the separation and property evaluation of isomerically pure ADTs. This class of amide functionalized ADT acceptors features high  $V_{oc}$  (> 1 V) in P3HT based solar cells and 0.8% PCE has been achieved.

This work was supported by the Office of Naval Research (grants N00014-05-1-0019 and N00014-11-10328). Y.-F. Lim acknowledges a research fellowship from A\*STAR, Singapore.

## Notes and references

† Crystallographic data for **syn-ADTA**:  $T = 90.0(2)$  K,  $C_{51}H_{60}N_2O_2S_2Si_2$ ,  $M = 853.31$ , triclinic space group  $P\bar{1}$ ,  $a = 11.1843(3)$  Å,  $b = 14.8367(4)$  Å,  $c = 15.7732(4)$  Å,  $\alpha = 63.054(1)^\circ$ ,  $\beta = 77.064(1)^\circ$ ,  $\gamma = 89.140(1)^\circ$ ,  $V = 2262.72(10)$  Å<sup>3</sup>,  $Z = 2$ , reflections collected/obs 8163/7758,  $R(\text{int}) = 0.0451$ ,  $R_1(\text{all data}) = 0.0365$ ,  $R_1(\text{obs}) = 0.0351$ . **Anti-ADTA**:  $T = 90.0(2)$  K,  $C_{44}H_{52}N_2O_2S_2Si_2$ ,  $M = 761.18$ , monoclinic space group  $P2_1/c$ ,  $a = 10.6703(3)$  Å,  $b = 16.2068(4)$  Å,  $c = 12.0490(3)$  Å,  $\beta = 106.683(1)^\circ$ ,  $V = 1995.94(9)$  Å<sup>3</sup>,  $Z = 2$ , reflections collected/obs 3647/3522,  $R(\text{int}) = 0.0564$ ,  $R_1(\text{all data}) = 0.0498$ ,  $R_1(\text{obs}) = 0.0470$ .

- J. J. M. Halls, C. A. Walsh, N. C. Greenham, E. A. Marseglia, R. H. Friend, S. C. Moratti and A. B. Holmes, *Nature*, 1995, **376**, 498–500; G. Yu, J. Gao, J. C. Hummelen, F. Wudl and A. J. Heeger, *Science*, 1995, **270**, 1789–1791.
- K. M. Coakley and M. D. McGehee, *Chem. Mater.*, 2004, **16**, 4533–4542; P. W. M. Blom, V. D. Mihailetschi, L. J. A. Koster and D. E. Markov, *Adv. Mater.*, 2007, **19**, 1551–1566.

- J. W. Chen and Y. Cao, *Acc. Chem. Res.*, 2009, **42**, 1709–1718.
- F. Padinger, R. S. Rittberger and N. S. Sariciftci, *Adv. Funct. Mater.*, 2003, **13**, 85–88; G. Li, V. Shrotriya, J. S. Huang, Y. Yao, T. Moriarty, K. Emery and Y. Yang, *Nat. Mater.*, 2005, **4**, 864–868.
- H. J. Son, W. Wang, T. Xu, Y. Y. Liang, Y. Wu, G. Li and L. P. Yu, *J. Am. Chem. Soc.*, 2011, **133**, 1885–1894; T. Y. Chu, J. P. Lu, S. Beaupr, Y. G. Zhang, J. R. Pouliot, S. Wakim, J. Y. Zhou, M. Leclerc, Z. Li, J. F. Ding and Y. Tao, *J. Am. Chem. Soc.*, 2011, **133**, 4250–4253; S. C. Price, A. C. Stuart, L. Q. Yang, H. X. Zhou and W. You, *J. Am. Chem. Soc.*, 2011, **133**, 4625–4631.
- J. C. Hummelen, B. W. Knight, F. Lepeq, F. Wudl, J. Yao and C. L. Wilkins, *J. Org. Chem.*, 1995, **60**, 532–538.
- M. L. Wienk, J. M. Kroon, W. J. H. Verhees, J. Knol, J. C. Hummelen, P. A. van Hal and R. A. J. Janssen, *Angew. Chem., Int. Ed.*, 2003, **42**, 3371–3375; M. Lenes, G. J. A. H. Wetzelaer, F. B. Kooistra, S. C. Veenstra, J. C. Hummelen and P. W. M. Blom, *Adv. Mater.*, 2008, **20**, 2116–2119; Y. J. He, H. Y. Chen, J. H. Hou and Y. F. Li, *J. Am. Chem. Soc.*, 2010, **132**, 1377–1382.
- J. E. Anthony, *Chem. Mater.*, 2011, **23**, 583–590.
- T. Kietzke, H. H. Horhold and D. Neher, *Chem. Mater.*, 2005, **17**, 6532–6537; X. W. Zhan, Z. A. Tan, B. Domercq, Z. S. An, X. Zhang, S. Barlow, Y. F. Li, D. B. Zhu, B. Kippelen and S. R. Marder, *J. Am. Chem. Soc.*, 2007, **129**, 7246–7247.
- J. J. Dittmer, E. A. Marseglia and R. H. Friend, *Adv. Mater.*, 2000, **12**, 1270–1274; J. L. Li, F. Dierschke, J. S. Wu, A. C. Grimsdale and K. Mullen, *J. Mater. Chem.*, 2006, **16**, 96–100; W. S. Shin, H. H. Jeong, M. K. Kim, S. H. Jin, M. R. Kim, J. K. Lee, J. W. Lee and Y. S. Gal, *J. Mater. Chem.*, 2006, **16**, 384–390.
- R. Y. C. Shin, T. Kietzke, S. Sudhakar, A. Dodabalapur, Z. K. Chen and A. Sellinger, *Chem. Mater.*, 2007, **19**, 1892–1894; Z. E. Ooi, T. L. Tam, R. Y. C. Shin, Z. K. Chen, T. Kietzke, A. Sellinger, M. Baumgarten, K. Mullen and J. C. Demello, *J. Mater. Chem.*, 2008, **18**, 4619–4622; R. Y. C. Shin, P. Sonar, P. S. Siew, Z. K. Chen and A. Sellinger, *J. Org. Chem.*, 2009, **74**, 3293–3298.
- P. Sonar, G. M. Ng, T. T. Lin, A. Dodabalapur and Z. K. Chen, *J. Mater. Chem.*, 2010, **20**, 3626–3636.
- F. G. Brunetti, X. Gong, M. Tong, A. J. Heeger and F. Wudl, *Angew. Chem., Int. Ed.*, 2010, **49**, 532–536.
- J. E. Anthony, J. S. Brooks, D. L. Eaton and S. R. Parkin, *J. Am. Chem. Soc.*, 2001, **123**, 9482–9483; M. M. Payne, S. R. Parkin, J. E. Anthony, C. C. Kuo and T. N. Jackson, *J. Am. Chem. Soc.*, 2005, **127**, 4986–4987; M. T. Lloyd, A. C. Mayer, A. S. Tayi, A. M. Bowen, T. G. Kasen, D. J. Herman, D. A. Mourey, J. E. Anthony and G. G. Malliaras, *Org. Electron.*, 2006, **7**, 243–248; M. T. Lloyd, A. C. Mayer, S. Subramanian, D. A. Mourey, D. J. Herman, A. V. Bapat, J. E. Anthony and G. G. Malliaras, *J. Am. Chem. Soc.*, 2007, **129**, 9144–9149; S. Subramanian, S. K. Park, S. R. Parkin, V. Podzorov, T. N. Jackson and J. E. Anthony, *J. Am. Chem. Soc.*, 2008, **130**, 2706–2707.
- C. R. Swartz, S. R. Parkin, J. E. Bullock, J. E. Anthony, A. C. Mayer and G. G. Malliaras, *Org. Lett.*, 2005, **7**, 3163–3166.
- Y. F. Lim, Y. Shu, S. R. Parkin, J. E. Anthony and G. G. Malliaras, *J. Mater. Chem.*, 2009, **19**, 3049–3056; Y. Shu, Y. F. Lim, Z. Li, B. Purushothaman, R. Hallani, J. Kim, S. R. Parkin, G. G. Malliaras and J. E. Anthony, *Chem. Sci.*, 2011, **2**, 363–368.
- O. D. Jurchescu, S. Subramanian, R. J. Kline, S. D. Hudson, J. E. Anthony, T. N. Jackson and D. J. Gundlach, *Chem. Mater.*, 2008, **20**, 6733–6737.
- B. Wex, B. R. Kaafarani, R. Schroeder, L. A. Majewski, P. Burckel, M. Grell and D. C. Neckers, *J. Mater. Chem.*, 2006, **16**, 1121–1124; T. Qi, Y. L. Guo, Y. Q. Liu, H. X. Xi, H. J. Zhang, X. K. Gao, Y. Liu, K. Lu, C. Y. Du, G. Yu and D. B. Zhu, *Chem. Commun.*, 2008, 6227–6229; S. Shinamura, I. Osaka, E. Miyazaki, A. Nakao, M. Yamagishi, J. Takeya and K. Takimiya, *J. Am. Chem. Soc.*, 2011, **133**, 5024–5035.
- C. J. Brabec, A. Cravino, D. Meissner, N. S. Sariciftci, T. Fromherz, M. T. Rispen, L. Sanchez and J. C. Hummelen, *Adv. Funct. Mater.*, 2001, **11**, 374–380.
- W. J. Potscavage, S. Yoo and B. Kippelen, *Appl. Phys. Lett.*, 2008, **93**, 193308.